The 2018 Structures Congress (Structures18)
Songdo Convensia, Incheon, Korea, August 27 - 31, 2018

Axial Load Behaviors of PSRC Composite Columns with Anchor-Type Transverse Reinforcements

*Hyeon-Jin Kim[1)] and Hong-Gun Park[2)]

[1),2)] *Department of Architectural Engineering, SNU, Seoul, 08826, Korea*
[1)] bultanun2@gmail.com

ABSTRACT

A concentric axial loading test was performed on PSRC column specimens to verify the axial load-carrying capacity. The primary test parameters were width-to-thickness ratio of steel angles, configuration and connection-detail of transverse reinforcements. The test results showed that the load-carrying capacity of the columns was less than the prediction according to AISC 360-16, because the normal strength cover concrete failed earlier than yielding of the high-strength steel angle. Closely spaced transverse reinforcements improved lateral confinement effect on core concrete, which increased the load-carrying capacity of the PSRC column specimens. Slender section-steel angles (with large width-to-thickness ratio) were vulnerable to local buckling after cover concrete spalling, which decreased the load-carrying capacity of the PSRC column specimens.

1. INTRODUCTION

To improve the structural capacity and constructability, a prefabricated steel-reinforced concrete (PSRC) column was developed. In the previous PSRC column [**Fig. 1**(a)], steel angles are placed at the corners of the cross section, and the steel angles are integrated using bolt-connection with transverse steel plates. By using bolt-connection between the steel angle and transverse plate, overall constructability and fabrication quality can be better. Further, the headed bolt can increase bond resistance between steel angle and concrete, which enables steel-concrete composite action.

Kim et al. (2016) performed concentric and eccentric axial loading tests on the PSRC columns with bolt-connected steel angles. The test results showed that the axial load-carrying capacity of the PSRC columns was comparable to that of conventional concrete-encased steel (CES) composite columns with the wide flange steel at the center of the cross section. In large eccentricity of axial load, the compressive strength of the PSRC columns was even greater than that of conventional CES columns, due to

[1)] Graduate Student
[2)] Professor

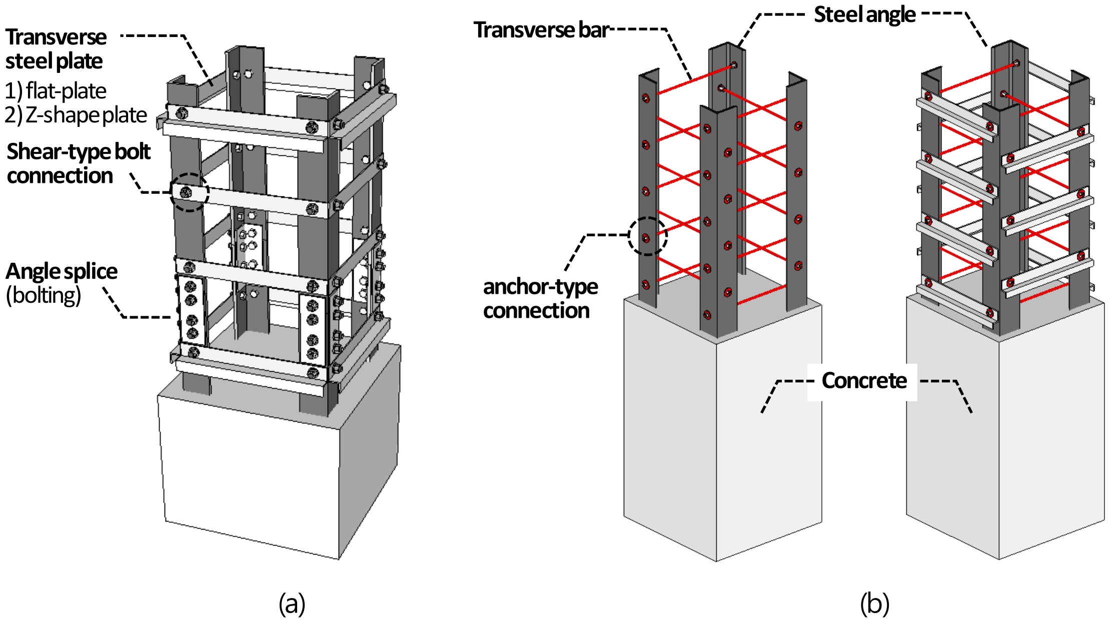

Fig. 1 PSRC composite columns using (a) bolt-connected transverse steel plates and (b) anchor-type transverse bars

high axial contribution of the corner-located steel angle. However, after the peak strength, the PSRC columns were vulnerable to spalling of cover concrete, due to the bond-failure between steel angles and concrete. Z-shaped transverse plates confined cover concrete, which prevented significant cover concrete spalling.

Despite the advantages of the bolt-connected PSRC columns, bolt-connection between steel angles and transverse plate requires significant design cost, especially in large-scale PSRC columns, due to various failure modes of the connection. Further, bolt-holes in steel angles decrease the effective net area of the steel angle, which reduces axial resistance of the steel angle.

In the proposed PSRC column [**Fig. 1**(b)], transverse bars are anchored to steel angles in the out-of-plane direction, which significantly simplifies the design of the steel angle-transverse bar connection. The transverse bars are alternately placed in x- and y-directions of the cross section, which reduces the sectional loss of the steel angles in the cross section. For a more reliable performance, the combination of Z-shaped transverse plates and transverse bars can be used.

To verify the structural capacity of the novel PSRC columns, concentric axial loading test was performed on six column specimens including a conventional PSRC column using bolt-connection. The axial load-carrying capacity of the columns was investigated, and compared with the prediction according to AISC 360-16.

2. TEST PLAN

2.1 Design of test specimens

Table 1 and **Fig. 2** show the geometric and material properties of PSRC column specimens **S1**-**S6**. The test parameters were the spacing of transverse reinforcements (120 mm and 200 mm), the width-to-thickness ratio of steel angles (7.2 for L-65x65x9 and 11.4 for L-80x80x7), and configuration of transverse reinforcements. The dimensions of the cross section were 400 x 400 mm, and the clear height of the column specimens was 1200 mm. The steel ratio of the specimens was the same as 2.7%.

To verify the applicability of high strength steel, the steels with yield strengths of F_y = 713 MPa and 732 MPa were used for the steel angles L-80x80x7 and L-65x65x9, respectively. The yield strengths of transverse steel plates (flat-shaped and Z-shaped) and transverse bar were F_y = 347 MPa and 513 MPa, respectively. The compressive strength of concrete at the day of column testing was 33.9 MPa.

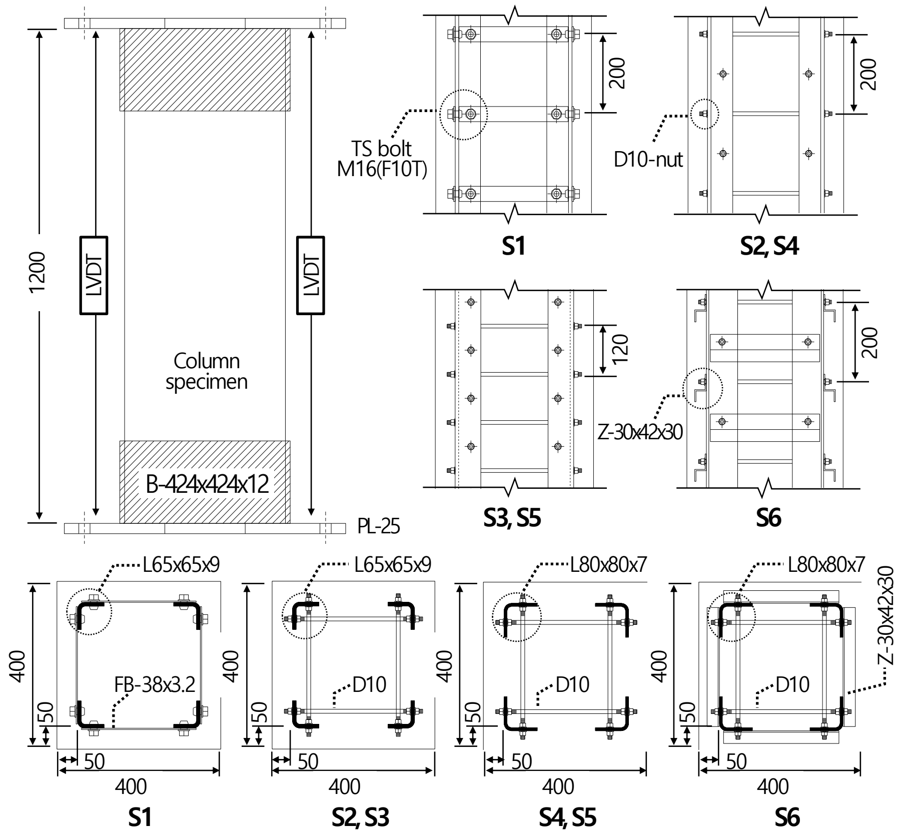

Fig. 2 Column specimens

Table 1. Test parameters of specimens

Specimens	S1	S2	S3	S4	S5	S6
Dimensions	Section width = 400 mm / Clear height = 1200 mm					
Vertical steel	L-65x65x9 (F_y = 732 MPa)			L-80x80x7 (F_y = 713 MPa)		
Transverse reinf. (yield strength)	FB38x3.2 (347 MPa) @200 mm	Bar-D10 (513 MPa) @200 mm	Bar-D10 (513 MPa) @120 mm	Bar-D10 (513 MPa) @200 mm	Bar-D10 (513 MPa) @120 mm	Bar-D10, Z-30x42x30 (513 MPa, 347

						MPa) @200 mm

2.2 Test and measurement setting

Axial load was applied by a 10MN-UTM, to the top of the column specimens. The specimens were directly supported on the rigid test bed. Axial loading was terminated at 60% of the peak strength of the column. Axial deformation of the columns was measured by vertical LVDTs installed at the four corners of the column.

3. TEST RESULTS

3.1 Axial load – strain relationship

Fig. 3 shows the axial load-strain (P-ε) relationships of the column specimens. The axial strain was calculated by dividing the average displacement measured from the LVDTs by the clear column height (=1200 mm). The peak strength P_u, axial strain

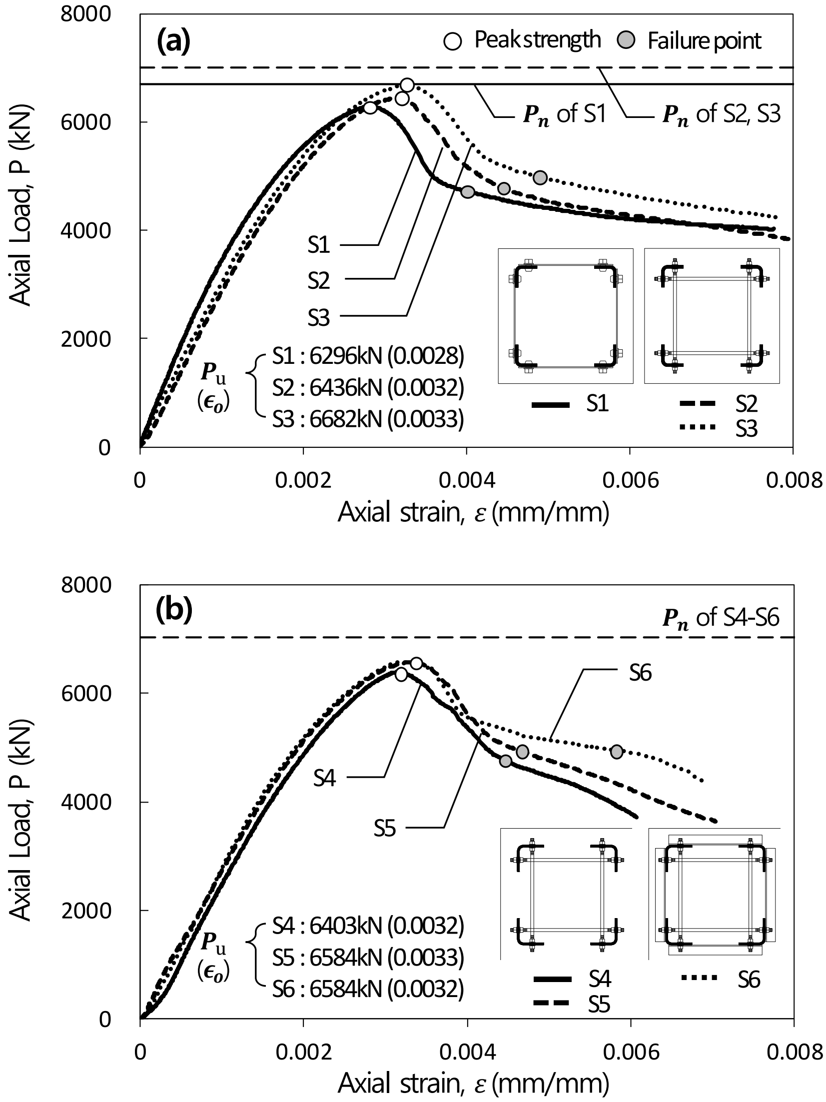

Fig. 3 Axial load-strain relationships of specimens

ε_0 corresponding to P_u, elastic stiffness K_e, ultimate strain ε_u, and nominal compressive strength P_n, and strength ratio P_u/P_n of the specimens are summarized in **Table 2**. The elastic stiffness K_e was defined as the slope corresponding to 0.75P_u (Park 1988), and the ultimate strain was defined as the post-peak strain corresponding to 0.75P_u (Eom et al. 2013).

As shown in **Fig. 3**, the peak strengths of the specimens were less than the predictions P_n by AISC 360-16 (horizontal solid and dotted lines). This is because the high strength steel angles did not yield even after the cover concrete failed. The strength ratios for the specimens were P_u/P_n = 0.91~0.95.

In PSRC specimens **S2**-**S6** with anchor-type transverse bars, the peak strength P_u, axial strain ε_o corresponding to P_u, elastic stiffness K_e, and ultimate strain ε_u were greater than those of bolt-connected PSRC specimen **S1**. This is partly because, in **S1**, effective sectional area of the steel angle in the cross section was small relative to that of **S2**-**S6**, which reduces the overall axial resistance of the column.

In **S3** and **S5** with transverse bars at a spacing of 120 mm, the peak strength P_u was greater than that of **S2** and **S4** with transverse bars at a spacing of 200mm, due to the improved lateral confinement. In **S4** and **S5** with slender section-steel angle, the peak strength P_u was slightly less than (or comparable to) that of **S2** and **S3** with nonslender section-steel angle. This result indicates that the premature buckling of the slender section-steel angle could be prevented until the cover concrete failed. In **S6**, by using combined transverse bars and Z-shaped plates, the load-carrying capacity was comparable to **S5**, even though the tie spacing of **S6** was greater than that of **S5**. On the other hand, due to the confinement effect of the Z-shaped plate, the deformation capacity (ultimate strain) was significantly improved.

In **S4**-**S6** with slender section-steel angles, post-peak degradation was greater than that of **S1**-**S3**, due to the structural instability (i.e., local buckling or out-of-plane deformation) of the steel angle after cover concrete spalling.

Table 2. Test results and prediction

Specimens	Test result				Prediction	
	P_u (kN)	ε_o (mm/mm)	K_e (kN/mm)	ε_u (mm/mm)	P_n (kN)	P_u / P_n
S1	6296	0.0028	2566	0.0034	6702	0.94
S2	6436	0.0032	2859	0.0038	7016	0.92
S3	6682	0.0033	2590	0.0048	7016	0.95
S4	6403	0.0032	2832	0.0037	7037	0.91
S5	6584	0.0033	2588	0.0043	7037	0.94
S6	6584	0.0032	2688	0.0041	7037	0.94

3.2 Failure modes

Fig. 4 shows the damages of cover concrete at the end of the test (60% of peak strength P_u). For all specimens, vertical cracks were prominent due to horizontal

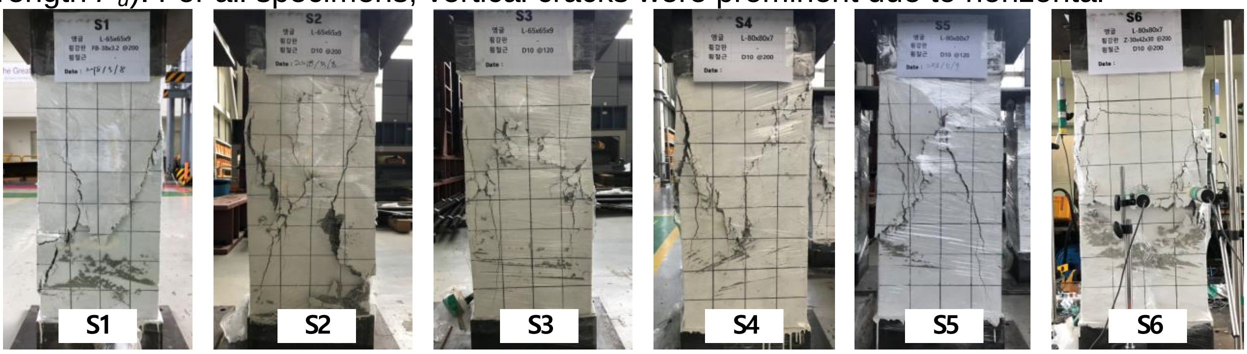

Fig. 4 Concrete damage at the end of the tests

expansion of concrete. However, the difference of the damage patterns between the specimens was not clear. Particularly, in **S6**, the cracking and spalling of cover concrete were relatively delayed until the failure point (=0.75P_u), due to the confinement effect of Z-shaped transverse plates.

4. SUMMARY AND CONCLUSIONS

In the present study, to investigate the structural capacity of PSRC columns with anchor-type transverse reinforcements, concentric axial loading tests were performed. From the test results, the load-carrying capacity, deformation capacity, and failure mode were investigated. The primary test results are summarized as follows:

(1) The deformation and load-carrying capacity of the PSRC columns using anchor-type transverse bars were greater than those of the PSRC column using bolt-connection between steel angles and transverse plates, due to high axial resistance of the steel angle.

(2) The axial load-carrying capacity of PSRC column specimens using normal strength concrete and high strength steel angles was less than the prediction according to AISC 360-16, due to the early failure of concrete before yielding of the steel angle. For a reliable performance corresponding to current design codes, further study on PSRC specimens using both high strength steel and concrete should be performed.

(3) Closely spaced transverse bars and Z-shaped transverse plates slightly increased the load-carrying capacity of the columns, due to the improved lateral confinement on concrete. Particularly, Z-shaped transverse plates prevented significant cover concrete damage even after the failure strength of the column.

(4) The local buckling of slender section-steel angles (with a width-to-thickness ratio of 11.4) did not occur until the cover concrete failed. However, after the cover concrete spalling, the load-carrying capacity of the specimens using the slender section-steel angles much decreased relative to the specimens using the nonslender section-steel angle, due to the local buckling and out-of-plane deformation of the steel angle.

REFERENCES

AISC. (2016), “Specification for structural steel building.”, *ANSI/AISC 360-16*, Chicago.

Eom, T.S., Hwang, H.J., Park H.G., Lee, C.N., Kim, H.S. (2013), “Flexural test for steel-concrete composite members using prefabricated steel angles.*” J. Struct. Eng.*, Vol. **140**(4), 04013094.

Kim et al. (2016), “Axial load test of prefabricated composite columns using bolt-connected steel angles.”, Journal of Korean Society of Steel Construction, Vol.**29**(2)

Kim et al. (2016), “Eccentric axial load test of prefabricated composite columns using bolt-connected steel angles.”, Journal of Korean Society of Steel Construction, Vol.**29**(3)

Park, R. (1988), “State-of-the-art report on ductility evaluation from laboratory and analytical testing.” *Proceedings of 9th World Conference on Earthquake Engineering*, Tokyo.